Four-Wave Mixing Analysis of Quantum Dot and Quantum Well Lasers

Hung-Hsin Lin, Chih-Hao Lin, and Fan-Yi Lin*

Institute of Photonics Technologies, Department of Electrical Engineering,
National Tsing Hua University,
Hsinchu 30013, Taiwan

ABSTRACT

In this paper, we characterize and compare a quantum dot and a quantum well lasers using the four-wave mixing analysis. The optical and power spectra of the four-wave mixing state in the quantum dot laser are studied both numerically and experimentally. The tendency of the amplitude versus detuning in the quantum dot laser is very similar to those seen in the quantum well laser. The four-wave mixing signals and the power spectra from both lasers are symmetric, while asymmetry in the regenerated signal is found. Compared to the quantum well lasers, the higher resonance peak of the regenerated signal of the quantum dot lasers appears on the opposite side of the detuning in the optical spectra. The intrinsic parameters of the lasers are also obtained by fitting the optical spectra and power spectra obtained experimentally with those derived directly from the rate equations. The measured value of the linewidth enhancement factor has a good agreement with that obtained by the injection locking method.

Keywords: Four-wave mixing, quantum dot laser, linewidth enhancement factor

1. INTRODUCTION

In recent years, nonlinear dynamics and their applications[1–4] of both quantum dot and quantum well semiconductor lasers have been studied extensively. The dynamical behaviors of these lasers are significantly influenced by the intrinsic laser parameters such as the linewidth enhancement factor. The linewidth enhancement factor of quantum dot lasers can be measured with many methods. The published methods of measuring the α-factor can be divided into two categories. First is the material α, which is the α-factor below the threshold current and is usually measured by the analysis of the amplified spontaneous emission (ASE).[5] The other is the device α, which is the α-factor above the threshold. The most commonly used methods are the FM/AM response ratio under small signal current modulation,[6] the linewidth measurement,[7] and the injection locking method.[7–10]

However, the FM/AM method is limited by the electric parasitic effects, while the calibration of the photo detector affects the measured result extremely. The principle of the linewidth measurement is to compare the linewidth measured below and above the threshold current, which is limited by the measuring range. The injection locking technique provides some ways for detecting α. One can measure the output power[10] or the junction voltage variation[8] under different detunings to extract the value of α. Moreover, the α-factor can also be measured from the slope ratio of the upper and the lower locking boundaries.[9] However, the power or voltage variation is small and the injection strength must be strong enough to get the accurate locking bandwidths. Differing from those methods which only measure the α-factor of the semiconductor lasers, four-wave mixing analysis can measure not only the α-factor but also other intrinsic parameters simultaneously.[11] The intrinsic parameters of semiconductor lasers affect the nonlinear dynamical characteristics considerably.[12] Furthermore, the relaxation resonance frequency can also be directly obtained from the optical spectra of the four-wave mixing.

In this paper, we apply the four-wave mixing analysis on quantum dot lasers and compare the measured α-factor with that obtained by the injection locking method. This comparison can be used to determine the degree of accuracy of each method.

Further author information: (Send correspondence to Fan-Yi Lin)
Fan-Yi Lin: E-mail: fylin@ee.nthu.edu.tw, Telephone: +886 3 5162185

Physics and Simulation of Optoelectronic Devices XIX, edited by Bernd Witzigmann, Fritz Henneberger, Yasuhiko Arakawa, Alexandre Freundlich, Proc. of SPIE Vol. 7933, 79331K · © 2011 SPIE · CCC code: 0277-786X/11/$18 · doi: 10.1117/12.873757

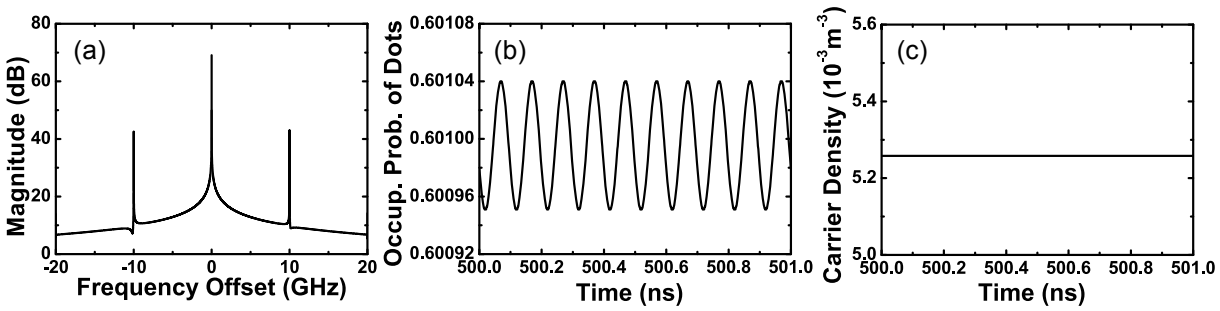

Figure 1. Simulated FWM state of the QD laser. (a) Optical spectrum of the laser output, (b) time series of the occupancy probability of the quantum dots, and (c) time series of the carrier density in the wetting layers.

2. MODEL AND METHOD

The dynamics of QD lasers with optical injection can be described by the rate equations for the complex amplitude of electric field E, the occupancy probability of the quantum dots ρ, and the carrier density in the wetting layers N_W.[13]

$$\frac{dE}{dt} = \frac{1}{2}v_g g_0 \left(\frac{2\rho - 1}{1 + \epsilon |E|^2} - \frac{\gamma_s}{v_g g_0} \right) (1 - i\alpha) E + E_i e^{-i\Delta t} \tag{1}$$

$$\frac{d\rho}{dt} = -\gamma_d \rho + C N_W (1 - \rho) - v_g \zeta \left(\frac{2\rho - 1}{1 + \epsilon |E|^2} \right) |E|^2 \tag{2}$$

$$\frac{dN_W}{dt} = -\gamma_N N_W + \frac{J}{q} - 2C N_W (1 - \rho), \tag{3}$$

where γ_s is the photon decay rate in the cavity, γ_N and γ_d are the carrier decay rates in the quantum wells and in the quantum dots, respectively. C is the capture rate from the quantum wells into the dot, J is the bias current per dot, ζ is the interaction cross section of the carriers in the dot with the electric field, α is the linewidth enhancement factor, Δ is the detuning frequency, v_g is the group velocity, g_0 is the differential gain, ϵ is the gain saturation coefficient, and E_i is the effective complex amplitude of the injected field. These rate equations are simplified[14,15] while have good agreement with the experimental result.[13]

The equations above are used to analyze the QD lasers through the four-wave mixing states. By deriving the equations of E, ρ, and N_W, the steady-state solutions of the rate equations at the FWM state can be obtained. Figure 1(a) shows the simulation results of the optical spectrum. The four-wave mixing state of the QD lasers is composed of three components: the free-oscillating signal, the regenerated amplification signal, and the FWM signal. Therefore, the output field can be expressed as

$$E(t) = E_0 + E_r e^{-i\Delta t} + E_f e^{i\Delta t}, \tag{4}$$

where E_0 is the steady-state field amplitude at the oscillating frequency, and E_r and E_f are the complex amplitudes of the regenerated amplification and FWM fields, respectively. The time series of the occupancy probability of the quantum dots ρ is shown in Fig. 1(b), which oscillates at the detuning frequency and thus can be described as

$$\rho(t) = \rho_0 + \rho_1 e^{-i\Delta t} + \rho_1^* e^{i\Delta t}, \tag{5}$$

where ρ_0 is the steady-state occupancy probability of the quantum dots without perturbation and ρ_1 is the amplitudes of the pulsation.

Figure 1(c) shows the time series of the carrier density in the wetting layers N_W. The N_W is nearly constant ($\simeq N_0$), where N_0 is the steady-state solution of N_W without perturbation. Therefore, we can set Eq. 3 equals to zero to get the free-running solution, which gives

$$N_W = \frac{J/q}{\gamma_N + 2C(1 - \rho)}. \tag{6}$$

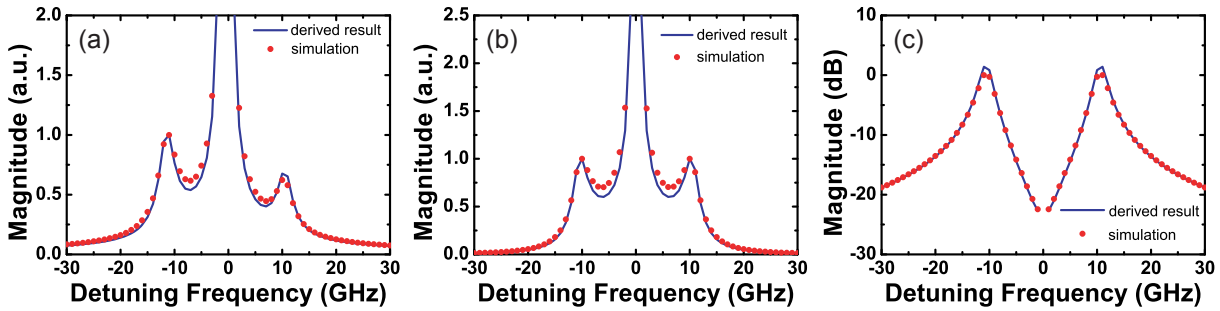

Figure 2. Comparison of the derived results and the simulated results. (a) Regenerated signal, (b) four-wave mixing signal, and (c) power spectra.

To simplify the calculation, we make some approximations based on the simulation results. First, the complex amplitude of the amplitude modulation (σ) is much smaller than the steady-state field amplitude (E_0), which gives

$$|E|^2 \approx |E_0|^2 \left(\sigma e^{-i\Delta t} + \sigma^* e^{i\Delta t}\right) \tag{7}$$

and

$$\frac{1}{1+\epsilon |E|^2} \approx \frac{1}{1+\epsilon |E_0|^2}. \tag{8}$$

Because the capture rate from the quantum wells into the dot (C) is generally much larger than the carrier decay rates in the quantum wells (γ_N) and the occupancy probability of the quantum dots (ρ) is in the range from 0 to 1, Eq. 6 can be reduced to

$$N_W = \frac{J/q}{2C(1-\rho)}. \tag{9}$$

By solving the steady-state solutions and substituting Eqs. 4, 5, and 9 into the rate equations, the complex amplitudes of the regenerative field, the FWM field, and the amplitude modulation versus the detuning frequency are obtained.

$$\frac{E_r}{E_0} = \frac{i\rho_1 G(1-i\alpha)}{\Delta} - K \tag{10}$$

$$\frac{E_f}{E_0} = \frac{i\rho_1^* G(1-i\alpha)}{\Delta} \tag{11}$$

$$\sigma = \rho_1 Z, \tag{12}$$

where

$$\rho_1 = \frac{-K}{Z+W}, G = \frac{v_g g_0}{1+\epsilon |E_0|^2}, K = \frac{-i}{\Delta}\frac{E_i}{E_0}, W = \frac{-i2G}{\Delta},$$
$$Z = \left[\frac{2v_g\zeta |E_0|^2}{1+\epsilon |E_0|^2} - i\Delta + \gamma_d\right] / \left[\frac{-v_g\zeta |E_0|^2 (2\rho_0 - 1)}{1+\epsilon |E_0|^2}\right]$$

Comparing these derived results with the simulated results in Fig. 2, we can see that the derived results roughly agree with the simulated results except for the point around the valleys. Thus, these results are confident and will be used to fit with the experiment results later. The used parameters are listed in Table 1.

3. EXPERIMENTAL SETUP

The schematic diagram of the experimental setup is shown in Fig. 3. The master laser is a tunable laser and the slave laser is a semiconductor quantum dot laser (QDLaser QLD 1334). The output of the master laser injects into the slave laser through the free space optical circulator composed of the polarizing beamsplitter,

Table 1. Used parameters in the QD rate equations

Parameters	Symbol	Value
Linewidth enhancement factor	α	4
Photon decay rate	γ_s	300 ns^{-1}
Carrier decay rates in the quantum wells	γ_N	1 ns^{-1}
Carrier decay rates in the quantum dots	γ_d	1 ns^{-1}
Capture rate from the quantum wells into the dots	C	1 ps^{-1}
Interaction cross section of the carriers	ζ	0.75 nm^2
Differential gain	g_0	90 cm^{-1}
Gain saturation coefficient	ϵ	2×10^{-22} m^{-3}

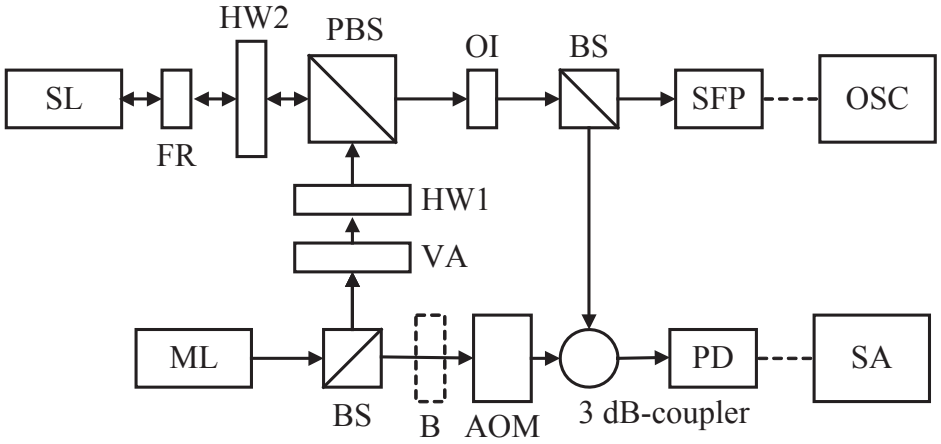

Figure 3. Schematic diagram of the experimental setup. FR: Faraday rotator; HW: half-wave plate; PBS: polarizing beamsplitter; OI: optical isolator; BS: beamsplitter; SFP: scanning Fabry-Perot interferometer; OSC: oscilloscope; PD: photodiode; SA: spectrum analyzer; VA: variable attenuator; AOM: acoustooptic modulator; B: beam block.

the half-wave plate 2, and the Faraday rotator. The four-wave mixing state can be observed with the scanning Fabry-Perot interferometer on the oscilloscope by adjusting the injection strength with the attenuator and the half-wave plate 1. The strength of the regenerated signal is obtained with heterodyne method. The output signal of the slave laser is received by a photodiode with 12 GHz frequency response (NewFocus 1554-A) and then coupled with the local oscillator signal. The local oscillator signal is the frequency-shifted injection light, where the frequency shifts 100 MHz after passing through an acousto-optical modulator (IntraAction ACM-1002AA1). The power spectra are obtained by measuring the output signal of the slave laser with a spectrum analyzer (Agilent E4407B).

4. RESULT AND DISCUSSION

The experimental results of the four-wave mixing analysis when the slave laser is biased at 1.5, 2, and 3 times of the threshold currents are shown in Fig. 4. Figures 4(a)-(c) present the optical spectra of the regenerated signal and Figs. 4(d)-(f) show the power spectra. The shapes of the measured optical spectra differ from the simulated results in the previous section, which are also different from the results typically seen in the quantum well lasers.[11] The discrepancy could result from the differences in the intrinsic parameters. Figure 5 shows the optical spectra of the regenerated signal and power spectra with different carrier decay rates in the dots. Other parameters are set as follow: linewidth enhancement factor ($\alpha = 2.5$), carrier decay rate in dots ($\gamma_d = 0.3$ ns^{-1}), the differential gain ($g_0 = 93$ cm^{-1}), the photon decay rate ($\gamma_s = 40$ ns^{-1}), the interaction cross section

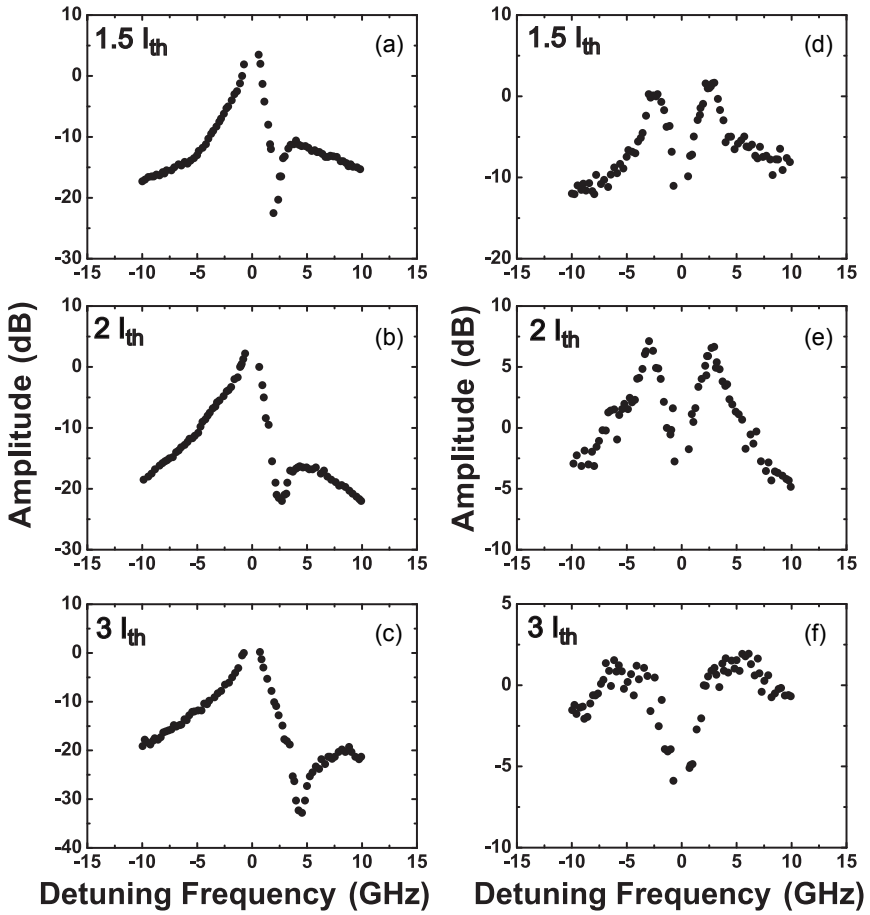

Figure 4. Experimental results of the FWM states for the QD laser. (a)-(c) The optical spectra and (d)-(f) the power spectra of the regenerated signals at 1.5, 2, and 3 times of the threshold current, respectively.

($\zeta = 0.78$ nm^2), the gain saturation coefficient ($\epsilon = 10.8 \times 10^{-22}$ m^{-3}), the capture rate from wells into dots ($C = 1$ ps^{-1}), and carrier decay rates in wells ($\gamma_N = 1$ ns^{-1}). As the carrier decay rate increases, the amplitude of the resonance peak decreases. If the carrier decay rate in the dots is fixed, similar results are observed as the differential gain increases. Notably, various values of other parameters will also affect the range of carrier decay rate and differential gain that make the resonance peak vanishes.

The fitting results of the four-wave mixing are shown in Fig. 6 and the obtained value of the parameters are listed in Table 2. The conditions that are applied to fit the experimental result with the derived equations are listed below. The linewidth enhancement factor (α), carrier decay rate in dots (γ_d), and the differential gain (g_0) are tuned with bias currents; the photon decay rate (γ_s), the interaction cross section (ζ), and the gain saturation coefficient (ϵ) are kept as constant among various bias current; other parameters barely affect the fitting result and thus are set as the same value used in Ref. 13. The errors shown in the table are dependent on the valley position at the positive detuning as shown in Fig. 7. From Refs. 16 and 17, the linewidth enhancement factor increases with bias current. In our fitting result, the linewidth enhancement factor is slightly increases as the bias current increases, but the variation is smaller than the error range. Therefore, the variation of the α-factor with the bias current is considered insignificantly.

The linewidth enhancement factor of the same laser is also extracted by using the injection locking technique for comparison.[10] Figure 8 shows the measured optical power variation with the QD laser biased at three times of the threshold current. The calculated value of the α-factor is 1.45 with an error of 0.17. The values of α-factor obtained from the injection locking and four-wave mixing analysis are similar. Therefore, applying four-wave

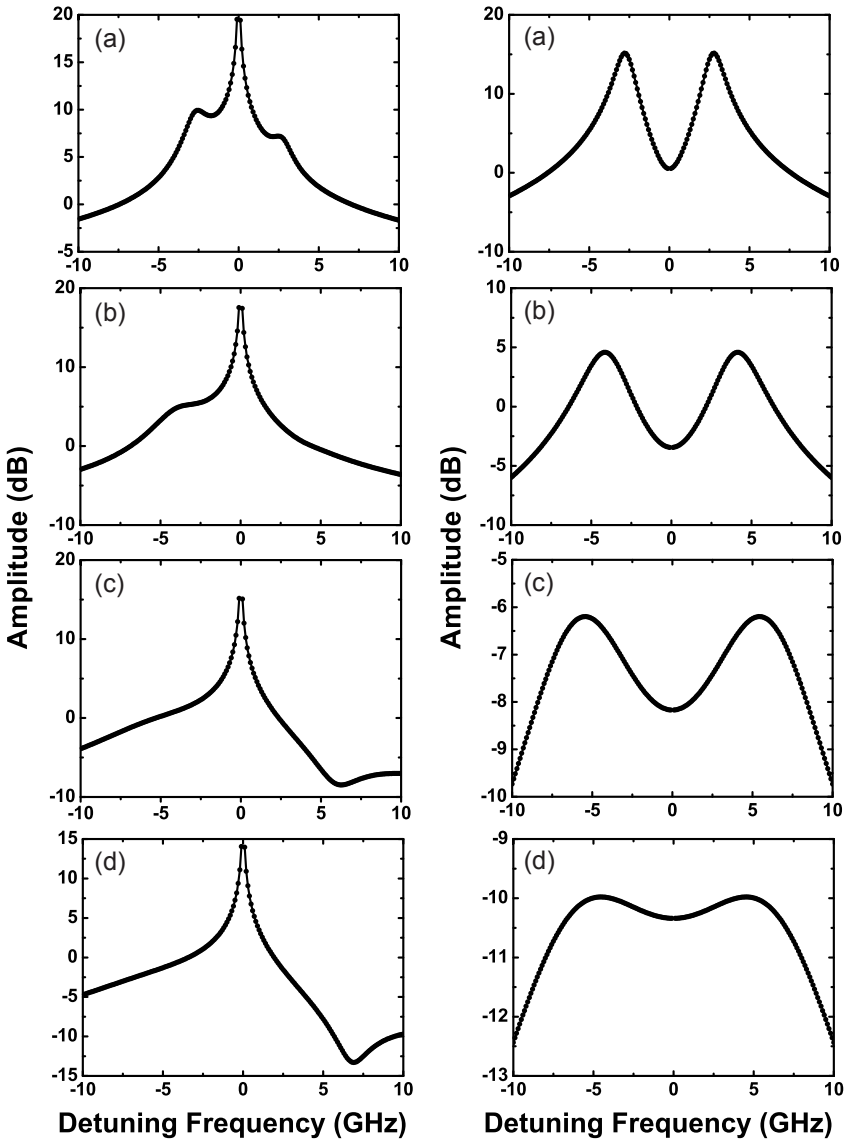

Figure 5. Simulated optical spectra (left column) and power spectra (right column) of the QD laser with different carrier decay rates in the dots. The carrier decay rates are (a) 0.2 ns^{-1}, (b) 0.5 ns^{-1}, (c) 1.5 ns^{-1}, and (d) 2.5 ns^{-1}.

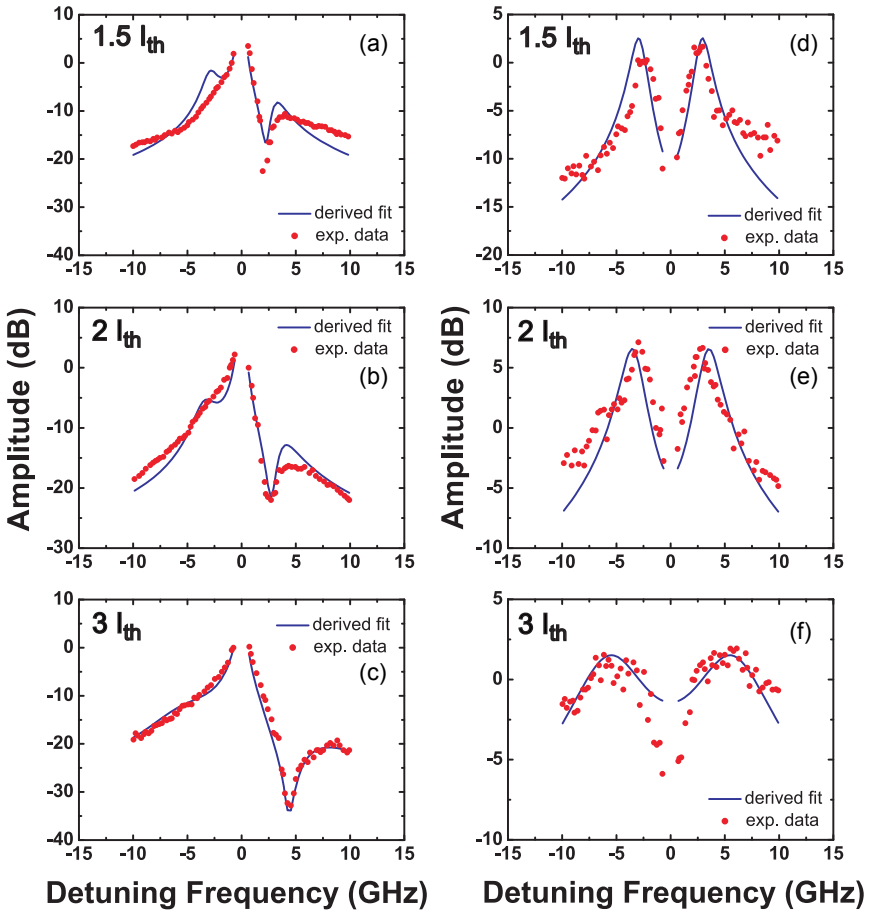

Figure 6. Fitting result of the FWM state for the QD laser. (a)-(c) present the optical spectra and (d)-(f) show the power spectra of the regenerated signals.

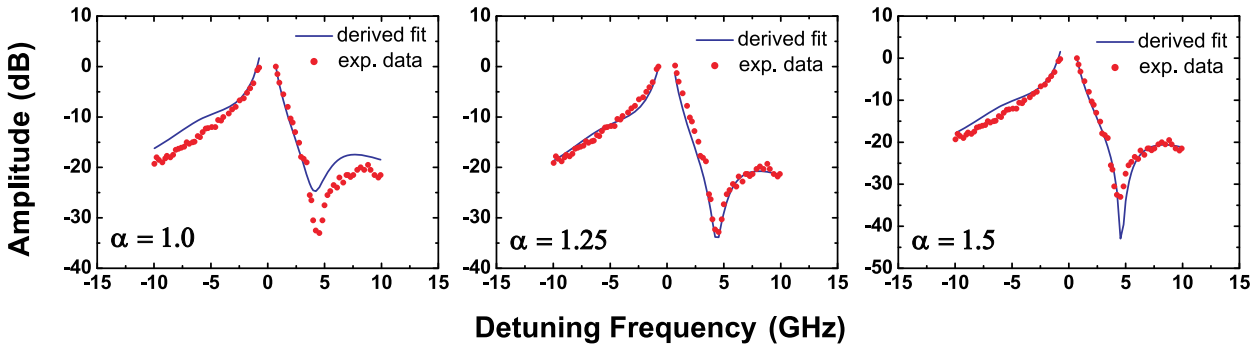

Figure 7. Example of the fitting error. QD laser is biased at the third times the threshold current and $\alpha = 1.25 \pm 0.25$.

Table 2. Fitting result of the intrinsic parameters in the QD laser.

Parameters	Unit	$1.5J_{th}$	$2J_{th}$	$3J_{th}$	Ref. 13
α	1	1.08 ± 0.4	1.18 ± 0.4	1.25 ± 0.25	2
γ_d	ns^{-1}	0.46 ± 0.2	0.45 ± 0.2	0.58 ± 0.2	1
g_0	cm^{-1}	93 ± 30	70 ± 30	101 ± 30	90
γ_s	ns^{-1}	40.1 ± 10	40.1 ± 10	40.1 ± 5	300
ζ	nm^2	0.78 ± 1	0.78 ± 1	0.78 ± 1	0.75
ϵ	10^{-22} m^{-3}	10.1 ± 10	10.1 ± 10	10.1 ± 10	2
γ_N	ns^{-1}	1	1	1	1
C	ps^{-1}	1	1	1	1

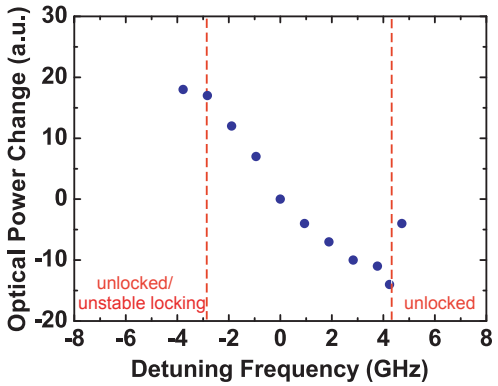

Figure 8. Experimental result of the injection locking method for the QD laser.

mixing analysis to measure the α-factor in QD lasers is proved to be practical.

5. CONCLUSION

We apply the four-wave mixing analysis to quantum dot lasers to extract the linewidth enhancement factor and other intrinsic parameters by fitting the experimental data of optical spectra and power spectra with those derived from the rate equations. The value of the linewidth enhancement factor agrees with that measured by the injection locking technique. Using four-wave mixing analysis, not only the linewidth enhancement factor but also other intrinsic parameters can be extracted simultaneously.

ACKNOWLEDGMENTS

This work is supported by the National Science Council of Taiwan under contract NSC 97-2112-M-007-017-MY3.

REFERENCES

1. F. Y. Lin, S. Y. Tu, C. C. Huang, , and S. M. Chang, "Nonlinear dynamics of semiconductor lasers under repetitive optical pulse injection," *IEEE J. of Sel. Top. Quantum Electron.* **15**(3), pp. 604–611, 2009.
2. Y. S. Juan and F. Y. Lin, "Demonstration of ultra-wideband (UWB) over fiber based on optical pulse-injected semiconductor laser," *Opt. Express* **18**(9), pp. 9664–9670, 2010.
3. W. T. Wu, Y. H. Liao, and F. Y. Lin, "Noise suppressions in synchronized chaos lidars," *Opt. Express* **18**(25), pp. 26155–26162, 2010.
4. Y. S. Juan and F. Y. Lin, "Microwave-frequency-comb generation utilizing a semiconductor laser subject to optical pulse injection from an optoelectronic feedback laser," *Opt. Lett.* **34**(11), pp. 1636–1638, 2009.

5. T. C. Newell, D. J. Bossert, A. Stintz, B. Fuchs, K. J. Malloy, and L. F. Lester, "Gain and linewidth enhancement factor in InAs quantum-dot laser diodes," *IEEE Phot. Tech. Lett.* **11**(12), pp. 1527–1529, 2002.
6. S. Gerhard, C. Schilling, F. Gerschutz, M. Fischer, J. Koeth, I. Krestnikov, A. Kovsh, M. Kamp, S. Hofling, and A. Forchel, "Frequency-Dependent Linewidth Enhancement Factor of Quantum-Dot Lasers," *IEEE Phot. Tech. Lett.* **20**(20), pp. 1736–1738, 2008.
7. T. Fordell and A. M. Lindberg, "Experiments on the Linewidth-Enhancement Factor of a Vertical-Cavity Surface-Emitting Laser," *IEEE J. Quantum Electron.* **43**(1), pp. 6–15, 2006.
8. R. Hui, A. Mecozzi, A. D'ottavi, and P. Spano, "Novel measurement technique of alpha factor in DFB semiconductor lasers by injection locking," *Electronics Letters* **26**(14), pp. 997–998, 2008.
9. I. Petitbon, P. Gallion, G. Debarge, and C. Chabran, "Locking bandwidth and relaxation oscillations of an injection-locked semiconductor laser," *IEEE J. Quantum Electron.* **24**(2), pp. 148–154, 2002.
10. K. Iiyama, K. Hayashi, and Y. Ida, "Simple method for measuring the linewidth enhancement factor of semiconductor lasers by optical injection locking," *Opt. Lett.* **17**(16), pp. 1128–1130, 1992.
11. J. M. Liu and T. B. Simpson, "Four-wave mixing and optical modulation in a semiconductor laser," *IEEE J. Quantum Electron.* **30**(4), pp. 957–965, 1994.
12. S. K. Hwang and J. M. Liu, "Dynamical characteristics of an optically injected semiconductor laser," *Opt. Commun.* **183**(1-4), pp. 195–205, 2000.
13. D. Goulding, S. P. Hegarty, O. Rasskazov, S. Melnik, M. Hartnett, G. Greene, J. G. McInerney, D. Rachinskii, and G. Huyet, "Excitability in a quantum dot semiconductor laser with optical injection," *Phys. Rev. Let.* **98**(15), p. 153903, 2007.
14. M. Sugawara, N. Hatori, H. Ebe, M. Ishida, Y. Arakawa, T. Akiyama, K. Otsubo, and Y. Nakata, "Modeling room-temperature lasing spectra of 1.3-μm self-assembled InAs/GaAs quantum-dot lasers: Homogeneous broadening of optical gain under current injection," *J. Appl. Phys.* **97**, p. 043523, 2005.
15. M. Gioannini, A. Sevega, and I. Montrosset, "Simulations of differential gain and linewidth enhancement factor of quantum dot semiconductor lasers," *Optical and Quantum Electronics* **38**(4), pp. 381–394, 2006.
16. S. Melnik, G. Huyet, and A. Uskov, "The linewidth enhancement factor α of quantum dot semiconductor lasers," *Opt. Exp.* **14**(7), pp. 2950–2955, 2006.
17. B. Dagens, A. Markus, J. X. Chen, J. G. Provost, D. Make, O. L. Gouezigou, J. Landreau, A. Fiore, and B. Thedrez, "Giant linewidth enhancement factor and purely frequency modulated emission from quantum dot laser," *Electronics Letters* **41**(6), pp. 323–324, 2005.